Extended treatment of charge response kernel comprising the density functional theory and charge regulation procedures

Tateki Ishida and Akihiro Morita

Citation: The Journal of Chemical Physics **125**, 074112 (2006); doi: 10.1063/1.2219746
View online: http://dx.doi.org/10.1063/1.2219746
View Table of Contents: http://aip.scitation.org/toc/jcp/125/7
Published by the American Institute of Physics

Extended treatment of charge response kernel comprising the density functional theory and charge regulation procedures

Tateki Ishida and Akihiro Morita[a)]
Department of Computational Molecular Science, Institute for Molecular Science, Myodaiji, Okazaki 444-8585, Japan

(Received 20 April 2006; accepted 12 June 2006; published online 21 August 2006)

We propose an extended treatment of the charge response kernel (CRK), $(\partial Q_a/\partial V_b)$, which describes the response of partial charges on atomic sites to external electrostatic potential, on the basis of the density functional theory (DFT) via the coupled perturbed Kohn-Sham equations. The present CRK theory incorporates regulation procedures in the definition of partial charges to avoid unphysical large fluctuation of the CRK on "buried" sites. The CRKs of some alcohol and organic molecules, methanol, ethanol, propanol, butanol, dimethylsulfoxide (DMSO), and tetrahydrofuran (THF) were calculated, demonstrating that the new CRK model at the DFT level has greatly improved the performance of accuracy in comparison with that at the Hartree-Fock level previously proposed. The CRK model was also applied to investigate spatial nonlocality of the charge response through alkyl chain sequences. The CRK model at the DFT level enables us to construct a nonempirical strategy for polarizable molecular modeling, with practical reliability and robustness. © *2006 American Institute of Physics*. [DOI: 10.1063/1.2219746]

I. INTRODUCTION

Electronic polarization in molecules plays an important role in intermolecular interaction in condensed phases. Electronic structure of molecules in solutions is distorted by the interaction with surrounding molecules, which in turn affects the electronic polarization and intermolecular interaction. The electronic polarization is also a source of many optical properties such as refractive index, Raman scattering, etc. In molecular modeling, procedures for treating the electronic polarization are classified into two types. First type is implicit treatment using nonpolarizable models of effective pairwise potentials which incorporate the polarization effect in condensed phase. SPC,[1] TIP3P,[2] or TIP4P (Ref. 2) models of water, for example, are categorized into this type. Second type is explicit treatment using polarizable molecular models.[3–8] Usually, the second type is more costly than the first type for the use of molecular dynamics (MD) calculation, but explicit electronic polarization is necessary to describe spatial or temporal fluctuation of electronic polarization, which is shown to be important in local solvation structure,[9] chemical reaction in solution,[10] interfaces,[11,12] etc.

One of the most useful treatments of the second type is to utilize an interaction site model which allows instantaneous redistribution of partial charges on the interaction sites. The charge redistribution is usually described by the chemical potential equilibration principle, and a number of fluctuating charge models have been developed based on this concept.[13–22] Those polarizable models can be readily implemented in usual classical MD simulations for practical use. However, these models require empirical parameters related to atomic electronegativity, hardness, etc., which have to be determined by some fitting procedures. Accordingly accurate empirical parametrization is crucial, and the parametrization should be carefully calibrated in a variety of molecules, molecular conformations, and environments.

The charge response kernel (CRK) theory provides another polarizable model based on the interaction site representation. The CRK, K_{ab}, is defined as

$$K_{ab} = \frac{\partial Q_a}{\partial V_b}, \tag{1}$$

where Q_a represents the partial charge at site a and V_b means the electrostatic potential at site b. This derivative quantity is utilized to represent the first-order response of the instantaneous charge Q_a as

$$Q_a = Q_a^0 + \sum_b^{\text{sites}} K_{ab} V_b, \tag{2}$$

where Q_a^0 is the partial charge at the site a of the isolated molecule. The idea of CRK originates from the charge sensitivity analysis based on the density functional theory,[23–25] while its formulation is rather different from other semiempirical models. We also note a related response quantity in the field of condensed matter physics, called the dynamical charge,[26] defined from the derivative of dipole moment with respect to atomic position. In the CRK model, K_{ab} is directly derived from the response theory of *ab initio* electronic structure, with no empirical parametrization involved. Its accuracy is therefore warranted by that of the underlying *ab initio* calculation. As another consequence of its nonempirical character, the CRK theory allows us to treat any molecular systems on the common footing via *ab initio* calculations, including different molecular conformers and even unstable radical species[27,28] that empirical parametrization is often difficult or cumbersome.

[a)]Electronic mail: amorita@ims.ac.jp

The CRK theory was first proposed at the Hartree-Fock (HF) level.[27] Since the CRK is defined from the derivative of wave function and thus closely related to the second derivative of the total energy, as will be explained in the next section, it can be computed via the coupled perturbed Hartree-Fock (CPHF) equations.[27] Subsequently the CRK on the basis of the Møller-Plesset second-order (MP2) perturbation level has been calculated by numerical differentiation.[29] While the CRK at the HF level was useful to discuss relative sensitivity of the charge polarization in a qualitative sense,[27] more accurate treatment of charge polarization is desired including electron correlation for practical use of molecular modeling. In principle, the CRK can be formulated at any level of electronic structure theory when the corresponding derivative theory is available. By employing a higher level, the accuracy of CRK is expected to be improved accordingly. In the present study, we propose the CRK on the basis of the density functional theory (DFT).

The DFT has been successfully applied to a number of chemical problems in the past decade.[24,30,31] In many systems the DFT calculations with widely used exchange-correlation functionals, such as B3LYP,[32,33] can achieve remarkable accuracy at a modest computational cost, almost equivalent to the HF calculations. Second derivative methods at the DFT level[34–38] have been developed using the coupled perturbed Kohn-Sham (CPKS) equations and applied to pertinent molecular properties such as frequency,[34,37] polarizability, and hyperpolarizability.[39,40] The CPKS formalism is employed also to analytically derive the CRK at the DFT level. The calculation of CRK could be carried out alternatively by numerical differentiation of the total energy (or the partial charge Q_a) with respect to the external potential V_b, but the analytical treatment via the CPKS equations has apparent advantage in terms of numerical accuracy and computational cost. This advantage is emphasized for large molecular systems.

In the definition of CRK in Eq. (1), the partial charges $\{Q_a\}$ are defined via least-squares fitting to the surrounding electrostatic potential outside a target molecule. Although the set of partial charges $\{Q_a\}$ thus determined are optimized to represent the intermolecular electrostatic interaction, we sometimes suffer from a fitting problem of partial charges on the "buried" sites in the molecule, where the surface area surrounding the site is not exposed.[19,41,42] The difficulty in defining partial charges on the buried sites could intrude on the CRK calculation based on the definition. As an example, this problem could cause unphysically large fluctuation of partial charges on the buried sites during a polarizable MD simulation with the CRK model. In the current study, we need to introduce regulation procedures for avoiding this problem, because we treat the solvent molecules which possess some buried carbon sites in alkyl groups. In Sec. II, we will describe the regulation procedures we introduced.

In the present paper, we apply the DFT version of the CRK to some representative solvent molecules. We select four solvents from alcohols: methanol, ethanol, propanol, and butanol, and two other organic solvents: dimethylsulfoxide (DMSO) and tetrahydrofuran (THF). These are used frequently as common solvents,[43] and therefore their molecular models will be of use for theoretical studies in solution chemistry. This set of molecules does not intend to be comprehensive but to exemplify the accuracy and reliability of the new CRK model. We note that the CRK theory is free from empirical parameters that should be optimized for a training set of systems.

This paper is organized as follows. Section II explains theoretical aspects of CRK, including the general formalism of CRK, its extension at the DFT level with the CPKS equations, and the charge regulation procedures. Section III describes computational details about the DFT calculations and the derivation of partial charges. In Sec. IV, the calculated results of CRK for the selected molecules are presented, and their quantitative accuracy is critically discussed. The series of alcohols is also discussed in terms of the effect of alkyl chain length on the charge polarization. Conclusion is given in Sec. V.

II. THEORY

In this section, first we briefly summarize the general theory of CRK using the wave function formalism, following Ref. 27, and the extension of CRK to the Kohn-Sham DFT follows in Sec. II B. Then the definition of partial charges will be improved in Sec. II C.

A. Charge response kernel and coupled perturbed Hartree-Fock equations

In the derivation of the CRK, K_{ab}, the perturbation Hamiltonian has to be defined. The system Hamiltonian including the perturbation is represented using the interaction site model as follows:

$$\hat{H} = \hat{H}_0 + \sum_a^{\text{sites}} \hat{Q}_a V_a, \tag{3}$$

where $\hat{H}_0$ means the zeroth order Hamiltonian of the isolated molecule, and the second term corresponds to the perturbation at the Hamiltonian $\hat{H}_0$. The partial charge operator $\hat{Q}_a$ is defined by the least-square fitting of the surrounding electrostatic potentials, as mentioned in Sec. I. The partial charge at site a, Q_a, is represented as

$$Q_a = \langle \Psi | \hat{Q}_a | \Psi \rangle, \tag{4}$$

$$\hat{Q}_a = \sum_i^{\text{elec}} \hat{q}_a(i) + Q_a^{\text{nuc}}, \tag{5}$$

where Ψ denotes the wave function of the system. $\hat{q}_a(i)$ is the one-electron operator of the ith electron, and Q_a^{nuc} is the contribution from nuclear charges. The definition of the partial charges will be discussed in detail in Sec. II C. When the Hellmann-Feynman theorem is fulfilled, we note that Q_a and K_{ab} are given as the first and second derivatives of the total energy E, respectively,

$$Q_a = \frac{\partial E}{\partial V_a}, \quad K_{ab} = \frac{\partial^2 E}{\partial V_a \partial V_b}. \tag{6}$$

The CRK, K_{ab} in Eq. (1), is rewritten with the first derivative of the wave function Ψ^b with respect to V_b as follows;

$$K_{ab} = \frac{\partial Q_a}{\partial V_b} = \langle \Psi^b | \hat{Q}_a | \Psi \rangle + \langle \Psi | \hat{Q}_a | \Psi^b \rangle. \tag{7}$$

The derivative of the wave function has been formulated by the CPHF equation within the framework of *ab initio* theory,[44–46] which we briefly summarize in the closed-shell HF case in the following.[27]

Here, suffixes $p,q,\ldots$ refer to atomic orbitals (AOs), and $i,j,\ldots$ to molecular orbitals (MOs), and we suppose the MO coefficient and its derivative with respect to V_b are denoted by C_{pi} and C^b_{pi}, respectively,

$$\psi_i = \sum_p^{\mathrm{AO}} \chi_p C_{pi}, \quad \frac{\partial \psi_i}{\partial V_b} = \sum_p^{\mathrm{AO}} \chi_p C^b_{pi}, \tag{8}$$

and C_{pi} and C^b_{pi} are related with the transformation matrix U^b,

$$C^b_{qi} = \sum_j^{\mathrm{MO}} C_{qj} U^b_{ji}. \tag{9}$$

U^b is formulated by the following linear equations, called CPHF equations, in the closed-shell HF case,

$$(\epsilon_l - \epsilon_i) U^b_{li} + \sum_j^{\mathrm{occ}} \sum_k^{\mathrm{virt}} H^{(\mathrm{MO})}_{likj} U^b_{kj} = -q_{b,li}, \tag{10}$$

where i, j and k, l indicate the occupied and virtual MOs, respectively. $q_{b,li}=\langle l|\hat{q}_b|i\rangle$ is the matrix element of one-electron partial charge operator $\hat{q}_b$ in the MO representation. ϵ_i is the canonical orbital energy of the ith MO, and $H^{(\mathrm{MO})}$ is the two-electron integrals in the MO representation defined as

$$H^{(\mathrm{MO})}_{likj} = 4(li|kj) - (lk|ij) - (lj|ki). \tag{11}$$

Once Eq. (10) is solved, the CRK is derived as

$$K_{ab} = \sum_i^{\mathrm{occ}} \sum_l^{\mathrm{virt}} 4 q_{a,il} U^b_{li}. \tag{12}$$

B. Extension of CRK to density functional theory and coupled perturbed Kohn-Sham equation

The extension to the Kohn-Sham (KS) theory is fairly straightforward, by making use of the analogy between the KS and HF formalisms. In the following, we will focus on the differences between the two.

In the KS theory, a set of noninteracting orbitals, ϕ_i (KS orbitals),[24,31,47] is introduced, and the electron density ρ is thereby represented as

$$\rho = 2\sum_{i=1}^{N} |\phi_i|^2. \tag{13}$$

Here, we deal with a closed-shell system of $2N$ electrons. The DFT energy expression in the KS theory is written as

$$E_{\mathrm{DFT}}[\rho] = 2\sum_{i=1}^{N} h_{ii} + 2\sum_{i=1}^{N}\sum_{j=1}^{N} (ii|jj) + E_{\mathrm{xc}}[\rho], \tag{14}$$

where $h_{ii}=\langle i|\hat{h}|i\rangle$ indicates the one-electron integral consisting of noninteracting kinetic energy and nuclear attraction, the second term the Coulomb repulsion, and the third term $E_{\mathrm{xc}}[\rho]$ the exchange-correlation functional. Under the condition that the energy E_{DFT} is stationary, the following KS equation is derived to determine the KS orbitals:

$$\hat{F}^{\mathrm{KS}} \phi_i = \epsilon^{\mathrm{KS}}_i \phi_i. \tag{15}$$

The KS operator $\hat{F}^{\mathrm{KS}}$ is represented in the matrix form,

$$F^{\mathrm{KS}}_{pq} = \langle p|\hat{F}^{\mathrm{KS}}|q\rangle = h_{pq} + 2\sum_{i=1}^{N} (pq|ii) + V^{\mathrm{xc}}_{pq}[\rho], \tag{16}$$

where $V^{\mathrm{xc}}_{pq}[\rho]=\langle p|\delta E_{\mathrm{xc}}[\rho]/\delta\rho|q\rangle$. Note that $\delta E[\rho]/\delta\rho$ means functional differentiation. Using the KS orbitals thus obtained, the partial charge Q_a is given as

$$Q_a = 2\sum_{i=1}^{N} \langle i|\hat{q}_a|i\rangle + Q^{\mathrm{nuc}}_a. \tag{17}$$

Therefore, calculation of the CRK requires the derivative of the KS orbitals with respect to the external perturbation.

Then the external perturbation $\{V_a\}$ is applied. The one-electron operator $\hat{h}$ in Eq. (16) is modified to

$$\hat{h} = \hat{h}_0 \rightarrow \hat{h} = \hat{h}_0 + \sum_a^{\mathrm{sites}} \hat{q}_a V_a, \tag{18}$$

where $\hat{h}_0$ is the original one-electron operator including the kinetic energy and nuclear attraction, and the additional second term indicates the perturbation. The derivatives of the KS orbitals with respect to V_b written using the transformation matrix U^b in parallel with Eq. (9),

$$\frac{\partial \phi_i}{\partial V_b} = \sum_j^{\mathrm{MO}} \phi_j U^b_{ji}. \tag{19}$$

Then U^b is given by the following CPKS equations, analogous with Eq. (10),

$$(\epsilon^{\mathrm{KS}}_l - \epsilon^{\mathrm{KS}}_i) U^b_{li} + \sum_j^{\mathrm{occ}} \sum_k^{\mathrm{virt}} H^{\mathrm{KS}}_{likj} U^b_{kj} = -q_{b,li}, \tag{20}$$

where H^{KS}_{likj} involves the derivative of the exchange-correlation functional,

$$H^{\mathrm{KS}}_{likj} = 4(li|kj) + 4\left(lk \left| \frac{\delta^2 E_{\mathrm{xc}}[\rho]}{\delta\rho\delta\rho'} \right| ji \right), \tag{21}$$

where $(lk|\delta^2 E_{\mathrm{xc}}[\rho]/\delta\rho\delta\rho'|ji)=\langle k|\delta V^{\mathrm{xc}}_{li}[\rho]/\delta\rho|j\rangle$. The functional form of $\delta^2 E_{\mathrm{xc}}[\rho]/\delta\rho\delta\rho'$ depends on the exchange-correlation functional $E_{\mathrm{xc}}[\rho]$. In the case of employing hybrid functionals, where $E_{\mathrm{xc}}[\rho]$ consists of the exact exchange part and the pure DFT part $\phi_{\mathrm{xc}}[\rho]$ with mixing ratios of a and b,

$$E_{\mathrm{xc}}[\rho] = -a\sum_{i=1}^{N}\sum_{j=1}^{N}(ij|ij) + b\phi_{\mathrm{xc}}[\rho], \tag{22}$$

H_{likj}^{KS} is accordingly expressed as

$$H_{likj}^{\mathrm{KS}} = 4(li|kj) - a\{(lk|ij) + (lj|ki)\} + 4b\left(lk\left|\frac{\delta^2\phi_{\mathrm{xc}}[\rho]}{\delta\rho\delta\rho'}\right|ji\right). \tag{23}$$

The second derivative expression in Eq. (21) or (23) may be complicated but straightforward[34,36,38] once the form of $E_{\mathrm{xc}}[\rho]$ is given. In fact, H^{KS} is commonly used for DFT calculations of second derivative quantities, such as frequency or polarizability, and we readily implemented the CRK calculation by making use of the program code for other second derivative quantities. Using the solution of Eq. (20), the CRK is obtained via Eq. (12).

Finally, we note that the CRK is related to the dipolar polarizability as follows. The molecular dipole moment μ_i $(i=x,y,z)$ is given with the partial charges Q_a by

$$\mu_i = \sum_{a}^{\mathrm{sites}} Q_a R_i(a), \tag{24}$$

where $R_i(a)$ means the Cartesian coordinate of site a. Consequently, the molecular polarizability tensor α_{ij} is derived by taking the derivative of Eq. (24) with respect to the electric field E_j,

$$\alpha_{ij} = \frac{\partial\mu_i}{\partial E_j} \simeq \sum_{b}^{\mathrm{sites}} \frac{\partial\mu_i}{\partial V_b}\frac{\partial V_b}{\partial E_j} = -\sum_{a,b}^{\mathrm{sites}} K_{ab}R_i(a)R_j(b). \tag{25}$$

The accuracy of Eq. (25) will be confirmed in Sec. IV.

C. Charge regulation methods

In this subsection we discuss the definition of partial charges with the charge regulation procedures, as mentioned in Sec. I. First the general procedure to define the electrostatic potential (ESP) charges is briefly summarized, and then the two regulation procedures are introduced.

For the least-squares fitting of partial charges $\{Q_a\}$, the electrostatic potentials generated by the electrons of the molecule are evaluated at grid points distributed around the target molecule. The sum of the squared deviation L is

$$L = \sum_{n}^{\mathrm{grid}} w_n\left(-2\sum_{i=1}^{N}\left\langle i\left|\frac{1}{|\mathbf{R}^{\mathrm{grid}}(n)-\mathbf{r}|}\right|i\right\rangle + \sum_{c}^{\mathrm{nuc}}\frac{Z_c}{|\mathbf{R}^{\mathrm{grid}}(n)-\mathbf{R}^{\mathrm{nuc}}(c)|} - \sum_{a}^{\mathrm{sites}}\frac{Q_a}{|\mathbf{R}^{\mathrm{grid}}(n)-\mathbf{R}(a)|}\right)^2, \tag{26}$$

where $\mathbf{R}^{\mathrm{grid}}(n)$, $\mathbf{R}(a)$, $\mathbf{R}^{\mathrm{nuc}}(c)$, and $\mathbf{r}$ denote the coordinates of the grid point n, the interaction site a, the nucleus c, and the electron, respectively. (Note that interaction sites do not necessarily coincide with nuclear positions.) Z_c is the nuclear charge of the atom c. The distribution of the grid points $\mathbf{R}^{\mathrm{grid}}(n)$ will be discussed in Sec. III. Considering the minimization of L, the equations for $\{Q_a\}$ are

$$\frac{\partial}{\partial Q_a}\left\{L - 2\kappa\left(\sum_{b}^{\mathrm{sites}} Q_b - Q\right) - 2\boldsymbol{\xi}\cdot\left(\sum_{b}^{\mathrm{sites}} Q_b\mathbf{R}(b) - \boldsymbol{\mu}\right)\right\} = 0, \tag{27}$$

where κ and $\boldsymbol{\xi}$ are the Lagrange multipliers to introduce constraints on the total charge $Q=\Sigma_b^{\mathrm{sites}}Q_b$ and the dipole moment $\boldsymbol{\mu}$ in Eq. (24), respectively. Equation (27) leads to the following solution:

$$Q_a = \sum_{b}^{\mathrm{sites}} [\mathbf{A}^{-1}]_{ab}\{B_b + \kappa + \boldsymbol{\xi}\cdot\mathbf{R}(b)\}, \tag{28}$$

where $\mathbf{A}$ and $\mathbf{B}$ are represented as

$$A_{ab} = \sum_{n}^{\mathrm{grid}} w_n \frac{1}{|\mathbf{R}^{\mathrm{grid}}(n)-\mathbf{R}(a)|}\frac{1}{|\mathbf{R}^{\mathrm{grid}}(n)-\mathbf{R}(b)|}, \tag{29}$$

$$B_a = \sum_{n}^{\mathrm{grid}} w_n\left(-2\sum_{i=1}^{N}\left\langle i\left|\frac{1}{|\mathbf{R}^{\mathrm{grid}}(n)-\mathbf{r}|}\right|i\right\rangle + \sum_{c}^{\mathrm{nuc}}\frac{Z_c}{|\mathbf{R}^{\mathrm{grid}}(n)-\mathbf{R}^{\mathrm{nuc}}(c)|}\right)\frac{1}{|\mathbf{R}^{\mathrm{grid}}(n)-\mathbf{R}(a)|}. \tag{30}$$

We also note that $\mathbf{A}$ is symmetric and positive definite. L in Eq. (26) is represented in the matrix form as

$$L(\mathbf{Q}) = \mathbf{Q}^T\mathbf{A}\mathbf{Q} - 2\mathbf{Q}^T\mathbf{B} + \mathrm{const}. \tag{31}$$

The standard least square fitting, Eq. (27), is summarized to the following linear equation:

$$\mathbf{A}\mathbf{Q} - \mathbf{B}' = 0, \tag{32}$$

where

$$B_a' \equiv B_a + \kappa + \boldsymbol{\xi}\cdot\mathbf{R}(a). \tag{33}$$

1. Regulation method 1

The above standard procedure of least square fitting may lead to an ill-defined solution, when the $\mathbf{A}$ matrix has nearly zero eigenvalue(s). Then the displacement of $\mathbf{Q}$ along the corresponding eigenvector could become unphysically large, with little influence on the squared deviation L. This situation tends to occur when the target molecule has buried sites, as mentioned in Sec. I essentially because the partial charges of the buried sites are difficult to be evaluated outside the target molecule by shielding from neighboring sites. Therefore, it is required to regulate this troublesome eigenvalue distribution of $\mathbf{A}$. In the following, we propose two prescriptions for this problem.

As one of remedies for avoiding the above-mentioned instability, introducing a damping factor in the large eigenvalue(s) of the $\mathbf{A}^{-1}$ has been proposed (denoted as regulation method 1 below).[42] Suppose that the $\mathbf{A}$ matrix is diagonalized using a unitary matrix $\mathbf{P}$,

$$\mathbf{A} = \mathbf{P}^{\mathbf{T}}\cdot\mathbf{E}\cdot\mathbf{P}, \tag{34}$$

$$\mathbf{E} = \begin{pmatrix} e_1 & & \\ & \ddots & \\ & & e_n \end{pmatrix}, \quad 0 < e_1 < \cdots < e_n, \tag{35}$$

the modified inverse matrix $\mathbf{A}_{\mathrm{mod}}^{-1}$ is defined as follows;

$$\mathbf{A}_{\mathrm{mod}}^{-1} = \mathbf{P}^{\mathbf{T}} \cdot \mathbf{E}_{\mathrm{mod}}^{-1} \cdot \mathbf{P}, \tag{36}$$

$$\mathbf{E}_{\mathrm{mod}}^{-1} = \begin{pmatrix} 1/\sqrt{e_1^2 + \lambda_1^2} & & \\ & \ddots & \\ & & 1/\sqrt{e_n^2 + \lambda_1^2} \end{pmatrix}, \tag{37}$$

where $\lambda_1(>0)$ is the damping parameter. $\mathbf{Q}$ is then given from Eq. (28) by replacing $\mathbf{A}^{-1}$ with $\mathbf{A}_{\mathrm{mod}}^{-1}$ in Eq. (36). This modification could handle the instability caused by small eigenvalues e_i which are comparable to or smaller than λ_1.[42]

2. Regulation method 2

Another way to regulate the ill-posed matrix problem of $\mathbf{A}$ is to minimize the square of norm $\|\mathbf{AQ}-\mathbf{B}'\|^2$ with an auxiliary penalty function (denoted as regulation method 2). For more details for general treatment, readers should refer to the literature.[48,49]

The target function to be minimized, $S(\mathbf{Q})$, is set to

$$S(\mathbf{Q}) = \|\mathbf{AQ} - \mathbf{B}'\|^2 + \lambda_2^2 p(\mathbf{Q}), \tag{38}$$

where $p(\mathbf{Q})$ is the penalty function and λ_2 is a weight parameter for the penalty function. Here, $p(\mathbf{Q})$ is assumed to be a quadratic form of $\mathbf{Q}$ with unit kernel $\mathbf{I}$,

$$p(\mathbf{Q}) = \mathbf{Q}^T \mathbf{I} \mathbf{Q}. \tag{39}$$

The minimization condition, $\partial S(\mathbf{Q})/\partial \mathbf{Q} = 0$, leads to the following solution of $\mathbf{Q}$;

$$\mathbf{Q} = (\mathbf{AA} + \lambda_2^2 \mathbf{I})^{-1} \mathbf{AB}'. \tag{40}$$

It should be noted that this regulation method 2 is closely related to the method 1. Equation (40) means that $\mathbf{A}^{-1}$ in Eq. (28) is modified to

$$\mathbf{A}_{\mathrm{mod}(2)}^{-1} = (\mathbf{AA} + \lambda_2^2 \mathbf{I})^{-1} \mathbf{A}. \tag{41}$$

Accordingly, the diagonalized form of $\mathbf{A}_{\mathrm{mod}(2)}^{-1}$ in the regulation method 2 is given as

$$\mathbf{E}_{\mathrm{mod}(2)}^{-1} = \begin{pmatrix} e_1/(e_1^2 + \lambda_2^2) & & \\ & \ddots & \\ & & e_n/(e_n^2 + \lambda_2^2) \end{pmatrix}. \tag{42}$$

As we can see from Eqs. (37) and (42), both methods commonly modify small eigenvalues of $\mathbf{A}$ matrix in different ways.

The value of λ_1 or λ_2 can be determined from the eigenvalue distribution of the $\mathbf{A}$ matrix. In Sec. IV, we will apply both the regulation methods to the charge fitting calculation. We note that theory of CRK in Sec. II A or II B is not altered by the modified definition of the $\mathbf{A}$ matrix in either regulation.[42]

III. CALCULATION

In this section we describe the implementation and conditions of the CRK calculations.

The program code for the CRK calculation was implemented into the GAMESS-UK package.[50] We utilized the DFT module of the GAMESS-UK, including the CPKS equations, and convert it for use of the CRK calculations.[51] While the modified code is generally applied to CRK calculations with exchange-correlation functionals supported by GAMESS-UK, the following CRK calculations were performed using the B3LYP hybrid functional, the most widely used one for practical use. We have confirmed the implemented code for the CRK calculations in comparison with the numerical differentiation of partial charges. Also, we carried out the CRK calculation at the HF level for comparison.

The basis sets we employed for carbon, oxygen, and sulfur are *d*-aug-cc-pVTZ without *f* functions and diffuse *d* functions.[52–55] For sulfur, the exponents of the second diffuse set were given as $\alpha=0.018\,68$ for *s* and 0.011 22 for *p*, by even-tempered expansion. These exponents were generated from those of the first diffuse set of aug-cc-pVTZ by multiplying scaling factors, $\beta=0.3759$ for *s* and 0.3197 for *p*, which were determined for each angular momentum as the ratio of the exponents of the two most diffuse functions in aug-cc-pVTZ.[55] For hydrogen, the aug-cc-pVTZ set without *d* diffuse functions was employed.[52] Accordingly the qualities of the basis sets are characterized as $(12s7p2d)/[6s5p2d]$ for carbon and oxygen, $(17s11p4d)/[7s6p4d]$ for sulfur, and $(6s3p1d)/[4s3p1d]$ for hydrogen.

The geometry structures of all nine solvents were optimized by B3LYP and above basis sets using the GAUSSIAN 03 program,[56] prior to the CRK calculations. Optimization was carried out under C_s symmetry except for the three molecules, ethanol (*gauche*), 2-propanol, and 2-butanol, which were under C_1 symmetry. Alkyl chains of 1-propanol, 2-propanol, and 1-butanol are of all-trans conformation.

In the definition of partial charges, we put the interaction sites at all atomic nuclei. It should be noted that the atomic sites alone could not describe out-of-plane polarization by CRK for a flat or linear molecule,[27,28] but none of the molecules we used in this study are in the case. (In the modeling of flat or linear molecules, auxillary sites besides the atomic nuclei could be added to remove this deficiency.[29]) The fitting procedure for the partial charges was performed with the constraint on the total charge and the dipole moment,[42,57] as discussed in Sec. II C. The grid point distribution outside the molecule takes account of the molecular symmetry to make the fitted partial charges symmetry adopted. The weighting factor w_k in Eq. (26) for each grid point is commonly set to be 1 in the current study. The grid point distribution around each atomic nucleus was defined by the Lebedev grid generating methods.[58,59] These methods can avoid biasing grid points in certain angular directions around an atomic center. The details of the grid generation are given in the following.

For the distribution of the grid points, we begin by generating a sphere shell of radius 1 a.u. (=0.53 Å) around each atom and placing grids on the sphere shell by the Lebedev

TABLE I. The polarizability tensors of methanol and DMSO derived by Eq. (25) and by DFT calculation (unit in a.u.). z axis is set normal to the C_s plane. y axis is parallel to C–O in methanol, while x axis is parallel to S=O in DMSO.

	Model			DFT		
	x	y	z	x	y	z
			Methanol			
x	20.709 56			20.709 56		
y	−0.614 13	23.626 42		−0.614 13	23.626 42	
z	0.000 00	0.000 00	20.062 49	0.000 00	0.000 00	20.062 49
			DMSO			
x	54.545 68			54.545 68		
y	−5.273 84	49.384 55		−5.273 84	49.384 55	
z	0.000 00	0.000 00	59.302 24	0.000 00	0.000 00	59.302 24

method. Next, the radius is increased by 1 a.u. and a new sphere shell is generated with grids placed on it. This scheme is repeated until the distance from the center of atom is increased up to 20 a.u. for each atom. The distributed grid points on each shell follow the point group symmetry of the molecule. Then, the grid points generated within the distance equal to the standard atomic van der Waals radius[60] on the envelopes are removed. Also, considering the Voronoi region[61] of each atom, the points where overlap with grid points around different atomic sites were discarded. The total numbers of grid points N^{grid} amount to 7636 for methanol, 8797 for ethanol (trans), 8854 for ethanol (*gauche*), 9924 for 1-propanol, 9593 for 2-propanol, 11077 for 1-butanol, 10601 for 2-butanol, 9445 for DMSO, and 10269 for THF. The regulation parameters λ_1 and λ_2 in Sec. II C are optimized in the next section.

IV. RESULTS AND DISCUSSION

In this section, first we examine the calculated CRKs of the nine solvent molecules in terms of their dipole moments and polarizabilities, and experimentally available molecular properties for electronic polarization. The CRKs are then refined by introducing the charge regulations, and the consequent results are discussed. The CRK thus obtained is applied to a series of alcohol molecules to investigate the nonlocality of the charge redistribution.

A. Dipole moment and polarizability calculation

First we examine the ability of the present CRK model to describe dipole moment and polarizability. In this sense, there are two issues regarding the accuracy. One is the ability of the CRK model to reproduce the quantities obtained by the underlying DFT (or *ab initio*) calculations, and the other is the accuracy of the DFT calculations themselves employed for the CRK calculation. We briefly examine these issues in order below.

The present model gives the dipole moment vector and polarizability tensor by Eqs. (24) and (25), respectively. The dipole moment μ_i defined by Eq. (24) should necessarily coincide with that of the underlying DFT calculation because of the constraint condition in the least square fitting, whereas the polarizability given by Eq. (25) needs to be examined. This is because Eq. (25) evaluates the electric field only via the electrostatic potentials at the interaction sites. Therefore, Table I shows the comparison of the polarizability tensors directly computed by the DFT/B3LYP calculation with those by the CRK method via Eq. (25) at the same level for methanol and DMSO, showing excellent agreement between the two methods. These results indicate that the constraint on the dipole moment works well for the polarizability calculated with the CRK model. We note that the above calculations did not employ the charge regulation procedures in Sec. II but we found that the regulations influence little on the agreement.

Tables II and III display the dipole moments and isotropic polarizabilities calculated by Eqs. (24) and (25), respectively, for nine solvent molecules in comparison with experimental data. These tables also show the calculated results by the HF level with the same basis sets for comparison. As seen in the tables, the results with the DFT/B3LYP are substantially improved from those by the HF level.[31] It is well known that HF calculations tend to overestimate the dipole moment, and this tendency seems to remain to lesser extent in the present B3LYP results by ≈0.1–0.2 D. This deviation is partly attributed to the basis set we have employed.[31] The model polarizabilities at the DFT level show good accordance with the experimental data within about 0.4 Å^3. While

TABLE II. Dipole moments calculated by HF and B3LYP with Eq. (24) and their experimental values (unit in debye).

	HF	B3LYP	Expt.
Methanol	1.81	1.67	1.70±0.02,[a] 1.66[b]
Ethanol (trans)	1.73	1.59	1.44±0.03[a]
Ethanol (*gauche*)	1.86	1.73	1.68±0.03[a]
1-propanol	1.64	1.50	1.55±0.03 (trans)[a]
2-propanol	1.78	1.65	1.58±0.03[a]
1-butanol	1.70	1.57	1.66±0.03[a]
2-butanol	1.78	1.66	1.8 (liquid)[a]
DMSO	4.74	4.17	3.96±0.04[a]
THF	1.96	1.83	1.75±0.04[a]

[a]Reference 68.
[b]Reference 69.

TABLE III. Isotropic polarizabilities calculated by HF and B3LYP with Eq. (25) and their experimental values (Unit in Å^3).

	HF	B3LYP	Exp.
Methanol	2.900	3.181	3.29,[a] 3.23,[a] 3.32[a]
Ethanol (trans)	4.605	5.022	5.41,[a,c] 5.11[a,c]
Ethanol (*gauche*)	4.590	5.021	
1-propanol	6.291	6.823	6.74[a]
2-propanol	6.280	6.848	6.97,[a] 7.61[a]
1-butanol	8.009	8.673	8.88[a]
2-butanol	7.941	8.618	8.92[a]
DMSO	7.336	8.063	7.97[b]
THF	7.172	7.742	···

[a]Reference 68.
[b]Reference 70.
[c]Experimental values do not distinguish trans and gauche.

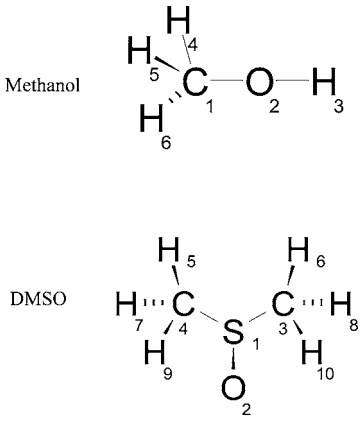

FIG. 1. Atomic site numbering of methanol and DMSO.

the experimental polarizability of tetrahydrofuran (THF) is not shown, the calculated result for THF is likely to be quantitatively close to the measurement if it would be carried out. In summary, the CRK theory at the DFT level allows for a substantially better model of electronic polarization. It is noted that the accuracy of CRK model does not depend on the ability of the model to reproduce the DFT calculation but on accuracy of the electronic structure calculation itself. We could improve the accuracy of CRK model by using better exchange-correlation functional and/or basis set.

B. Improvement of CRK by charge regulations

In contrast to the dipolar polarizability associated to long-range behavior of electrostatic potential, local charge response inside the molecule can be more difficult to be evaluated from the electrostatic potential outside the molecule. To circumvent the possible difficulty, two regulation procedures are introduced in Sec. II. Here, we discuss these regulation procedures in methanol and DMSO, which both involve buried carbon sites in the molecules. Note that the numberings of atomic sites are shown in Fig. 1.

Table IV shows the CRK matrix elements of methanol without charge regulation ($\lambda_1=0$ or $\lambda_2=0$). It is noteworthy that the magnitude of self-C1–C1 polarization ($\partial Q_{C1}/\partial V_{C1} \simeq -32.4$) is estimated about five times as large as that of self-O2–O2 polarization ($\partial Q_{O2}/\partial V_{O2} \simeq -6.5$). The C–H bond polarization of methyl group ($\partial Q_n/\partial V_{C1} \simeq 8.2-8.5$, n: H4, H5 and H6) is also emphasized more than the O–H bond polarization ($\partial H_3/\partial O_2 \simeq 2.7$). Table IV implies that the large

TABLE IV. Charge response kernel of methanol for no regulation, regulation method 1, and regulation method 2 (unit in a.u.).

	C1	O2	H3	H4	H5	H6
			No regulation			
C1	−32.406					
O2	8.301	−6.538				
H3	−0.878	2.687	−2.478			
H4	8.547	−1.646	0.223	−3.984		
H5	8.218	−1.402	0.223	−1.570	−4.504	
H6	8.218	−1.402	0.223	−1.570	−0.964	−4.504
			Regulation method 1			
C1	−4.875					
O2	1.267	−4.728				
H3	0.019	2.446	−2.438			
H4	1.440	0.140	0.013	−2.149		
H5	1.074	0.438	−0.020	0.278	−2.655	
H6	1.074	0.438	−0.020	0.278	0.885	−2.655
			Regulation method 2			
C1	−4.784					
O2	1.240	−4.739				
H3	0.024	2.459	−2.448			
H4	1.416	0.154	0.006	−2.145		
H5	1.052	0.443	−0.020	0.284	−2.649	
H6	1.052	0.443	−0.020	0.284	0.891	−2.649

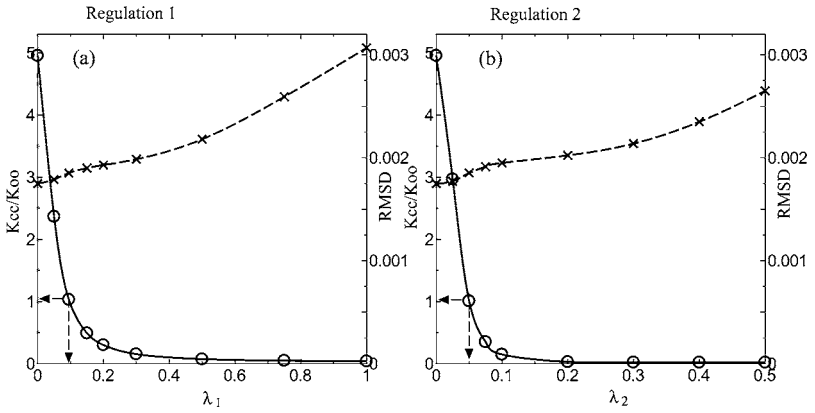

FIG. 2. Dependence of K_{CC}/K_{OO} and average RMSD on the λ parameters by (a) regulation method 1 and by (b) 2, as discussed in Sec. IV B. The circles mean K_{CC}/K_{OO} and the crosses are RMSDs. Note that the RMSDs are plotted to ordinates at the right side in each graph. The solid and dashed lines are for guiding eyes.

C1–C1 polarization is compensated by the large C–H polarizations, and consequently the lumped value in the methyl group $(\partial(Q_{C1}+Q_{H4}+Q_{H5}+Q_{H6})/\partial V_{C1} \simeq -7.5)$ is close to $\partial Q_{O2}/\partial V_{O2}$. These features indicate that the charge fluctuation at the C1 site is strongly coupled to the C–H bond polarization within the methyl group. Since the C1 carbon in the methyl group is considered to be a buried site, it is conceivable that the charge polarization within the methyl group is overestimated due to the instability problem of the partial charge fitting.

To examine this possible problem, we introduce the regulation procedures and calculate the CRK of methanol with varying parameter of λ_1 or λ_2. In either regulation method, the ratio of $\partial Q_{C1}/\partial V_{C1}$ to $\partial Q_{O2}/\partial V_{O2}$ $(=K_{CC}/K_{OO})$ and the average root-mean square deviation (RMSD) on the fitting accuracy, L/N^{grid}, are monitored with varying parameter λ. These results are depicted in Fig. 2, showing qualitatively analogous behaviors in the two regulation methods. With increasing λ_1 or λ_2 from zero, the ratio K_{CC}/K_{OO} is quickly damped from ~5 while the RMSD increases gradually. These results imply that the excessively large self-C1–C1 polarization relative to O2–O2 is controlled by a modest value of λ in either regulation method, with little influence on the charge fitting accuracy. This feature is indicative of the instability problem.

Next, we determine optimum values for the parameters λ_1 and λ_2. An optimum value should effectively correct the particularly large self polarization around the buried sites, with relatively small cost in the RMSD. Thus, we selected 0.095 for λ_1 and 0.05 for λ_2 (see Fig. 2) so that the self-C1–C1 polarization at the buried carbon is close to the O2–O2 self-polarization. These values of λ are also justified by the character of the **A** matrix in Eq. (29). The smallest eigenvalue of the **A** matrix in Eq. (35), $e_1=0.038$, is comparable in magnitude to the proposed values for λ_1 and λ_2 in the present system, indicating that these parameters control effectively the "source" of the instability in the charge fitting.[62] The CRKs of methanol thus optimized by two regulation methods are displayed also in Table IV. As shown in these tables, the two regulation procedures lead to similar results of CRK.

While the above regulations are able to correct large fluctuation around buried sites, the optimum values of λ_1 and λ_2 are somewhat arbitrary in terms of the charge fitting procedure for the electrostatic potentials outside the molecule. In order to confirm the validity of our regulation results, it is preferable to compare the present CRK model with other charge estimation methods regardless of the electrostatic potential outside the molecule on the buried sites. For this purpose, we employed two alternative charge estimation procedures, Mulliken and Ermler's population analysis[63] and natural population analysis (NPA),[64,65] which both partition the electron density into atoms of the target molecule in different ways. We "formally" estimated equivalent of charge response kernels by differentiating the Mulliken charges or the NPA charges with respect to the external electrostatic potentials $\{V_b\}$. For computing these equivalent quantities, the DFT calculations were carried out at the same conditions, and the differentiation was performed numerically with the five point formula. The Hamiltonian with external potential of Eq. (3) include the partial charge operator defined by the regulation method 2. With Mulliken and Ermler's population, $\partial Q_{C1}/\partial V_{C1}$, $\partial Q_{O2}/\partial V_{O2}$, and $\partial Q_{H4}/\partial V_{C1}$ are calculated to be −5.979 25, −4.107 78, and 2.080 08, respectively, and with the NPA, −2.082 80, −1.741 98, and 0.553 97, respectively. Consequently, $K_{CC}/K_{OO} \simeq 1.45$ for Mulliken and Ermler's population and ≃1.19 for the NPA. The results of K_{CC}/K_{OO} imply that the C1–C1 self-polarization should be comparable with the O2–O2 polarization, which is consistent to the regulated results of CRK with the optimum λ values. We note that the present CRK model does not necessarily coincide with the equivalent of Mulliken and Ermler's population or NPA, since the definition of partial charges is quite different. For purposes of representing intermolecular interactions, the CRK model based on the ESP charge is suitable.

The regulation methods also influence on the partial charges themselves. Table V summarizes the fitted partial charges of methanol. Comparing the partial charges with and without the regulations, we see that the C1 site is most sensitive to the regulations. The partial charge of 0.320 261 at C1 site is reduced to 0.086 272 by regulation 1 and 0.084 694 by regulation 2, while the residual charge is dis-

TABLE V. Site charges in methanol (unit in a.u.).

	C1	O2	H3	H4	H5	H6
No regulation	0.320	−0.612	0.367	0.010	−0.043	−0.043
Regulation 1	0.086	−0.557	0.362	0.065	0.022	0.022
Regulation 2	0.085	−0.558	0.363	0.066	0.022	0.022

TABLE VI. Charge response kernels and partial charges of DMSO (a) without regulation and (b) with regulation 2 (unit in a.u.).

		S1	O2	C3	C4	H5	H6	H7	H8	H9	H10
(a)	S1	−13.839									
	O2	4.006	−3.418								
	C3	10.459	−0.661	−43.403							
	C4	10.459	−0.661	1.825	−43.403						
	H5	−1.670	0.109	−1.247	11.450	−5.210					
	H6	−1.670	0.109	11.450	−1.247	0.866	−5.210				
	H7	−2.180	0.151	−1.398	12.721	−2.727	0.453	−5.749			
	H8	−2.180	0.151	12.721	−1.398	0.453	−2.727	1.021	−5.749		
	H9	−1.692	0.107	−0.233	10.486	−2.228	0.204	−2.506	0.214	−4.378	
	H10	−1.692	0.107	10.486	−0.233	0.204	−2.228	0.214	−2.506	0.025	−4.378
	Charge	0.201	−0.457	−0.072	−0.072	0.082	0.082	0.042	0.042	0.076	0.076
(b)	S1	−9.617									
	O2	3.632	−3.381								
	C3	1.329	0.194	−4.919							
	C4	1.329	0.194	0.372	−4.919						
	H5	0.761	−0.132	−0.408	1.131	−2.468					
	H6	0.761	−0.132	1.131	−0.408	0.501	−2.468				
	H7	0.332	−0.083	−0.434	1.612	0.237	0.075	−2.566			
	H8	0.332	−0.083	1.612	−0.434	0.075	0.237	0.618	−2.566		
	H9	0.570	−0.104	0.322	0.801	0.381	−0.078	0.328	−0.118	−1.976	
	H10	0.570	−0.104	0.801	0.322	−0.078	0.381	−0.119	0.328	−0.125	−1.976
	Charge	0.169	−0.455	0.014	0.014	0.057	0.057	0.018	0.018	0.054	0.054

tributed mainly to the methyl hydrogens, H4–H6. Table V also shows that the two regulation methods give similar values of partial charges. To examine the above partial charges of methanol, we can use the reported results by the restrained electrostatic potential (RESP) method[41] for comparison. The RESP charges on the methyl carbon site are 0.0569 and 0.1252 with the models 2 and 3 defined in the literature,[41] respectively. These values are consistent to the present charges on the C1 site, 0.085 and 0.086. These results indicate that the present regulation methods provide reasonable results of both partial charges and CRK.

As another example, we chose DMSO which possesses two methyl groups including buried carbon sites. In the discussion about methanol, it was found that our regulation methods effectively controlled the charge on the buried carbon site in methyl group. Therefore, we selected the same λ parameter value for each regulation as for methanol and checked whether our regulation works well also for DMSO. Table VI shows calculated partial charges and CRKs without regulation and with regulation method 2, where the atomic site numberings correspond to those in Fig. 1. It is noted that the regulation method 1 yields quite analogous results with regulation 2, and thus they are not shown. Comparing Table VIa and VIb to see the effect of regulation, differences in the diagonal CRK elements of C3–C3 and C4–C4 are conspicuous, −43.4 to −4.9, which correspond to the self-polarization of the methyl carbons. Accordingly, the CRK elements for the C–H bond polarizations within methyl groups (C3–H6, H8, H10 and C4–H5, H7, H9) are largely reduced from 10.5–12.7 to 0.8–1.6. The self-polarization of the buried methyl carbons, C3–C3 and C4–C4, after regulation becomes comparable to those of S1–S1 and O2–O2 and falls between the two [−9.6 for S1–S1, −3.4 for O2–O2 in Table VI(b)].

Finally, we note that the two regulation methods we proposed, so far, do not show large difference of performance. At present we can say both are promising. These methods will be examined via further application of the CRK model, including its conformational dependence.

C. Nonlocality of charge response in alkyl chains

In this subsection, we investigate the CRK matrix to discuss the extent of nonlocality in intramolecular polarization. The CRK model, $\partial Q_a/\partial V_b$, is suitable for this purpose, as it allows for general nonlocal response via any pair of sites, a and b, in the target system. The information on the nonlocality are also valuable for discussing transferability of the CRK model.

We choose a series of normal alcohols, $CH_3(CH_2)_nOH$ (n=0–3), as typical examples of alkyl chains, and observe the charge response on methyl ($-CH_3$) and methylene ($-CH_2-$) groups when imposing the electrostatic potential on the oxygen site of the terminal OH. Here the methyl/methylene moieties are labeled I, II, III,… in increasing order of distance from the terminal OH. The charge responses of methyl and methylene groups are evaluated by lumping the CRK elements of methyl or methylene sites, $\partial Q_i/\partial V_O$, where Q_i is the sum of partial charges within each methyl or methylene moiety, I, II, III, or IV. Among the series of alcohols, Fig. 3 shows that the self-polarization $\partial Q_O/\partial V_O$ is negative (∼−5), while the response at the adjacent group I changes its sign. The magnitude of the charge response decays with distance from the O site, though the sign is not

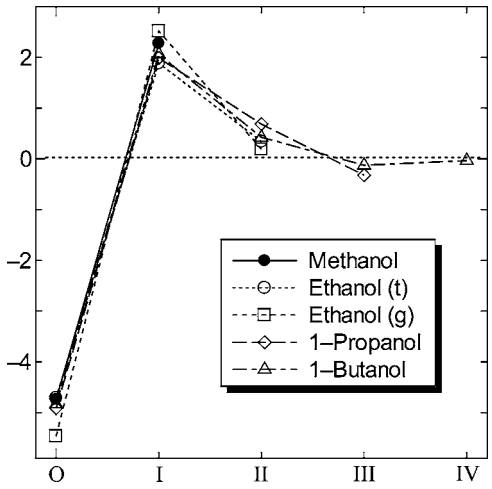

FIG. 3. Nonlocal charge response profiles, $\partial Q_i/\partial V_O$ (i=O,I,II,III,IV), of different alcohol molecules (see text in Sec. IV C).

necessarily constant. As seen in Fig. 3, the nonlocal profiles of the charge response show quite analogous behaviors among different chain lengths and trans/*gauche* conformers. The nonlocal charge response to the perturbation at the O site is reduced to less than 1/10 of the self O–O response through three single (C–C or C–O) bonds. The limited extent of the nonlocality through the alkyl chains could be utilized to extending the CRK model to larger systems including long alkyl chain sequences. The analogous nonlocal profiles should facilitate the transferability of the CRK model to other systems.

V. CONCLUSION

The charge response kernel (CRK), $\partial Q_a/\partial V_b$, defines the response quantity of partial charge Q_a to electrostatic potential V_b directly by *ab initio* or density functional calculations of molecules. Since this quantity is directly related to the response of electronic wave function or density, it is free from empirical parametrization to represent the electronic polarization. The nonempirical character of CRK facilitates its application as a general polarizable molecular modeling to a variety of molecules and conformers on the common footing. In the present paper, we extended the CRK model to the density functional theory (DFT). The response of the electron density was formulated via the coupled perturbed Kohn-Sham equations, similar to other response quantities such as frequency or polarizability.

In the CRK model, the partial charges $\{Q_a\}$ are defined from the electrostatic potential outside the target molecule. While the partial charges thus defined are suitable to describe intermolecular interaction, such procedures may be problematic to define charges at buried sites. This problem is circumvented by slightly modifying the definition of charges, introducing two regulation procedures. These modifications are fully compatible with the CRK theory.

We performed the CRK calculations by employing the B3LYP hybrid functional and sufficient basis sets including diffusive functions for some alcohols and organic molecules commonly used as solvents. Our calculation results indicated that the present treatment at the DFT level substantially improved the performance of accuracy over that at the Hartree-Fock level. In fact, the accuracy and reliability of the CRK are entirely determined by those of underlying electronic structure calculations. It is also confirmed that the two regulation procedures of partial charges yield reasonable and robust estimates of partial charges and CRK, by comparing them with other procedures for estimating partial charges. The CRK was also applied to elucidate spatial nonlocality of the charge response through alkyl chains.

In summary, the present CRK theory based on DFT can expand its applicability as a quantitatively reliable model of electronic polarization, including fairly large molecular systems. The CRK theory could be extended to incorporate polarization/exchange coupling[17,66,67] or charge-dependent response properties[18] in a nonempirical manner. Now the extension of CRK to modeling conformational isomers and application to studies on nonlinear optical spectroscopy are in progress.

ACKNOWLEDGMENTS

The authors thank Dr. K. Nakamura for comments on the work of dynamical charge method. This work was supported by the Grant-in-Aid and PETA Computing Grand-Challenge Project, MEXT, Japan.

[1] H. J. C. Berendsen, J. P. M. Postma, M. F. van Gunsteren, and J. Hermans, *Intermolecular Forces* (Reidel, Dordrecht, 1981).
[2] W. L. Jorgensen, J. Chandrasekhar, J. D. Madura, R. W. Impay, and M. L. Klein, J. Chem. Phys. **79**, 926 (1983).
[3] M. Sprik and M. L. Klein, J. Chem. Phys. **89**, 7556 (1988).
[4] J. A. C. Rullmann and P. T. van Juijnen, Mol. Phys. **63**, 451 (1988).
[5] P. Ahlström, A. Wallqvist, S. Engström, and B. Jönsson, Mol. Phys. **68**, 563 (1989).
[6] D. N. Bernardo, Y. B. Ding, K. K. Jespersen, and R. M. Levy, J. Phys. Chem. **98**, 4180 (1994).
[7] B. D. Bursulaya and H. J. Kim, J. Chem. Phys. **108**, 3277 (1998).
[8] A. E. Lefohn, M. Ovchinnikov, and G. A. Voth, J. Phys. Chem. B **105**, 6628 (2001).
[9] L. X. Dang, J. E. Rice, J. Caldwell, and P. A. Kollman, J. Am. Chem. Soc. **113**, 2481 (1991).
[10] R. Bianco and J. T. Hynes, *Solvent Effects and Chemical Reactivity* (Kluwer, Singapore, 1996).
[11] L. X. Dang, J. Chem. Phys. **110**, 10113 (1999).
[12] P. Jungwirth and D. J. Tobias, Chem. Rev. (Washington, D.C.) **106**, 1259 (2006).
[13] W. J. Mortier, S. K. Ghosh, and S. Shankar, J. Am. Chem. Soc. **108**, 4315 (1986).
[14] A. K. Rappe and W. A. Goddard, J. Phys. Chem. **95**, 3358 (1991).
[15] S. Rick, S. J. Stuart, and B. J. Berne, J. Chem. Phys. **101**, 6141 (1994).
[16] D. M. York and W. Yang, J. Chem. Phys. **104**, 159 (1996).
[17] T. J. Giese and D. M. York, J. Chem. Phys. **120**, 9903 (2004).
[18] T. J. Giese and D. M. York, J. Chem. Phys. **123**, 164108 (2005).
[19] J. L. Banks, G. A. Kaminski, R. Zhou, D. T. Mainz, B. J. Berne, and R. A. Friesner, J. Chem. Phys. **110**, 741 (1999).
[20] R. Chelli and P. Procacci, J. Chem. Phys. **117**, 9175 (2002).
[21] P. Bultinck, W. Langenaeker, P. Lahorte, F. De Proft, P. Geerlings, M. Waroquier, and J. P. Tollenaere, J. Phys. Chem. A **106**, 7887 (2002).
[22] P. Bultinck, W. Langenaeker, P. Lahorte, F. De Proft, P. Geerlings, C. Van Alsenoy, and J. P. Tollenaere, J. Phys. Chem. A **106**, 7895 (2002b).
[23] R. F. Nalewajski, *Chemical Hardness* (Springer-Verlag, Berlin, 1993).
[24] R. G. Parr and W. Yang, *Density-Functional Theory of Atoms and Molecules* (Oxford University, New York, 1989).
[25] P. Geerlings, F. De Proft, and W. Langenaeker, Chem. Rev. (Washington, D.C.) **103**, 1793 (2003).
[26] R. D. King-Smith and D. Vanderbilt, Phys. Rev. B **47**, 1651 (1993).
[27] A. Morita and S. Kato, J. Am. Chem. Soc. **119**, 4021 (1997).
[28] A. Morita and S. Kato, J. Chem. Phys. **108**, 6809 (1998).

[29] S. Iuchi, A. Morita, and S. Kato, J. Phys. Chem. B **106**, 3466 (2002).
[30] *Modern Density Functional Theory: A Tool for Chemistry*, edited by J. M. Seminario and P. Politzer (Elsevier, Amsterdam, 1995).
[31] W. Koch and M. C. Holthausen, *A Chemist's Guide to Density Functional Theory*, 2nd ed. (Wiley-VCH, Weinheim, 2000).
[32] A. D. Becke, J. Chem. Phys. **98**, 5648 (1993).
[33] C. Lee, W. Yang, and R. G. Parr, Phys. Rev. B **37**, 785 (1988).
[34] N. C. Handy, D. J. Tozer, G. J. Laming, C. W. Murray, and R. D. Amos, Isr. J. Chem. **33**, 331 (1993).
[35] A. Komornicki and G. Fitzgerald, J. Chem. Phys. **98**, 1398 (1993).
[36] B. G. Johnson and M. J. Frisch, J. Chem. Phys. **100**, 7429 (1994).
[37] R. E. Stratmann, J. C. Burant, G. E. Scuseria, and M. J. Frisch, J. Chem. Phys. **106**, 10175 (1997).
[38] H. van Dam, CCLRC Daresbury Laboratory Technical Report No. DL-TR-2001-002 (2001).
[39] A. M. Lee and S. M. Colwell, J. Chem. Phys. **101**, 9704 (1994).
[40] M. Kamiya, H. Sekino, T. Tsuneda, and K. Hirao, J. Chem. Phys. **122**, 234111 (2005).
[41] C. I. Bayly, P. Cieplak, W. D. Cornell, and P. A. Kollman, J. Phys. Chem. **97**, 10269 (1993).
[42] A. Morita and S. Kato, J. Phys. Chem. A **106**, 3909 (2002).
[43] J. A. Riddick, W. B. Bunger, and T. K. Sakano, *Organic Solvents*, 4th ed. (Wiley-Interscience, New York, 1986).
[44] J. Gerratt and I. M. Mills, J. Chem. Phys. **49**, 1719 (1968).
[45] P. Pulay, *Modern Electronic Structure Theory* (World Scientific, Singapore, 1995), Pt. II.
[46] J. A. Pople, R. Krishnan, H. B. Schlegel, and J. S. Binkley, Int. J. Quantum Chem., Symp. **13**, 225 (1979).
[47] W. Kohn and L. J. Sham, Phys. Rev. **140**, A1133 (1965).
[48] C. W. Groetsch, *Inverse Problems in the Mathematical Sciences*, 1st ed. (Friedrich, Wiesbaden, Germany, 1993).
[49] N. Tosaka, K. Onishi, and M. Yamamoto, *Mathematical Approach and Solution Methods for Inverse Problems: Inverse Analysis of Partial Differential Equations* (University of Tokyo Press, Tokyo, 1999).
[50] M. F. Guest, J. H. van Lenthe, R. D. Amos *et al.*, GAMESS-UK, a package of *ab initio* programs. The package is derived from the original GAMESS code due to M. Dupuis, D. Spangler and J. Wendoloski, NRCC Software Catalog, Vol. 1, Program No. QG01 (GAMESS), 1980.
[51] The initial DFT module within GAMESS-UK was developed by Dr. P. Young under the auspices of EPSRC's Collaborative Computational Project No. 1 (CCP1) (1995–1997). Subsequent developments have been undertaken by staff at the Daresbury Laboratory.
[52] T. H. Dunning, Jr., J. Chem. Phys. **90**, 1007 (1989).
[53] D. E. Woon and T. H. Dunning, Jr., J. Chem. Phys. **98**, 1358 (1993).
[54] R. A. Kendall, T. H. Dunning, Jr., and R. J. Harrison, J. Chem. Phys. **96**, 6796 (1992).
[55] D. E. Woon and T. H. Dunning, Jr., J. Chem. Phys. **100**, 2975 (1994).
[56] M. J. Frisch, G. W. Trucks, H. B. Schlegel *et al.*, GAUSSIAN 03, Revision C.01, Gaussian, Inc., Wallingford, CT, 2004.
[57] R. J. Woods, M. Khalil, W. Pell, S. H. Moffat, and J. V. H. Smith, J. Comput. Chem. **11**, 297 (1990).
[58] V. I. Lebedev, Zh. Vychisl. Mat. Mat. Fiz. **15**, 48 (1975).
[59] V. I. Lebedev, Sibirskii Matematicheskii Zhurnal **18**, 99 (1975).
[60] A. Bondi, J. Phys. Chem. **68**, 441 (1964).
[61] R. A. Friesner, J. Phys. Chem. **92**, 3091 (1988).
[62] Our previous paper (Ref. 42) proposed an optimum value of $\lambda_1(=\epsilon)$ to be 0.006. The difference in optimum value is attributed to different grid generation methods and thus **A** matrix. The optimum value depends on the eigenvalue distribution of the **A** matrix.
[63] R. S. Mulliken and W. C. Ermler, *Diatomic Molecules: Results of Ab Initio Calculation* (Academic, New York, 1977).
[64] A. E. Reed, R. B. Weinstock, and F. Weinhold, J. Chem. Phys. **83**, 735 (1985).
[65] A. E. Reed, L. A. Curtiss, and F. Weinhold, Chem. Rev. (Washington, D.C.) **88**, 899 (1988).
[66] A. Morita and S. Kato, J. Chem. Phys. **110**, 11987 (1999).
[67] A. Morita, J. Comput. Chem. **23**, 1466 (2002).
[68] *Handbook of Chemistry and Physics*, 85th ed., edited by D. R. Lide (CRC, Boca Raton, FL, 2004).
[69] *Kagaku Binran (Japanese)*, 5th ed. (Maruzen, Tokyo, 2004).
[70] K. J. Miller, J. Am. Chem. Soc. **112**, 8533 (1990).